

# Direct experimental impulse measurements for detonations and deflagrations

M. Cooper\*, S. Jackson<sup>†</sup>, J. Austin<sup>†</sup>, E. Wintenberger<sup>†</sup>, and J.E. Shepherd<sup>‡</sup>

*Graduate Aeronautical Laboratories,  
California Institute of Technology, Pasadena, CA 91125*

*Accepted to J. Propulsion and Power, Dec. 2001, revised June 15, 2002*

## Abstract

Direct impulse measurements were carried out by using a ballistic pendulum arrangement for detonations and deflagrations in a tube closed at one end. Three tubes of different lengths and inner diameters were tested with stoichiometric propane- and ethylene-oxygen-nitrogen mixtures. Results were obtained as a function of initial pressure and percent diluent. The experimental results were compared to predictions from an analytical model<sup>1</sup> and generally agreed to within 15%. The effect of internal obstacles on the transition from deflagration to detonation was studied. Three different extensions were tested to investigate the effect of exit conditions on the ballistic impulse for stoichiometric ethylene-oxygen-nitrogen mixtures as a function of initial pressure and percent diluent.

---

\*Graduate student, Mechanical Engineering

<sup>†</sup>Graduate student, Aeronautics

<sup>‡</sup>Professor, Aeronautics

## Nomenclature

$A_{TS}$	area of thrust surface
$A_{lip}$	area of lip at exit of tube
$c_2$	sound speed of burned gases just behind detonation wave
$c_3$	sound speed of burned gases behind Taylor wave
$d$	inner diameter of detonation tube
$F$	force exerted on detonation tube in direction of tube axis
$g$	standard earth gravitational acceleration
$I$	single-cycle impulse
$I_{sp}$	mixture-based specific impulse
$I_V$	impulse per unit volume
$L$	length of detonation tube filled with charge
$L_p$	length of pendulum arm
$L_t$	overall length of detonation tube and extension
$m$	pendulum mass
$p$	pitch of spiral obstacles
$P_1$	initial pressure of reactants
$P_2$	Chapman-Jouguet pressure
$P_3$	pressure of burned gases behind Taylor wave
$P_{env}$	environment pressure
$P_{lip}$	pressure on lip at exit of tube
$P_{TS}$	pressure on thrust surface in detonation tube interior
$S$	wetted surface area of tube's inner diameter
$T_1$	initial temperature of reactants
$U_{CJ}$	Chapman-Jouguet detonation velocity
$V$	internal volume of detonation tube
$\beta$	ratio of N <sub>2</sub> to O <sub>2</sub> concentration in initial mixture
$\Delta x$	horizontal pendulum displacement
$\gamma$	ratio of specific heats in combustion products
$\lambda$	cell size
$\rho_1$	density of combustible mixture at the initial temperature and pressure
$\tau$	wall shear stress

## Introduction

Impulse per cycle is one of the key performance measures of a pulse detonation engine. In order to evaluate the performance of the engine concept, it is necessary to have reliable

estimates of the maximum impulse that can be obtained from the detonation of a given fuel-oxidizer combination at a specified initial temperature and pressure. While the overall performance of an engine will depend strongly on a number of other factors such as inlet losses, nonuniformity of the mixture in the detonation tube, and the details (nozzles, extensions, coflow, etc.) of the flow downstream of the detonation tube exit, conclusive studies investigating the impulse available from a simple detonation tube must be completed. Many researchers have measured the impulse created by detonating a uniform mixture in a constant-area tube that is closed at one end and open at the other with a variety of experimental techniques.

The pioneering work measuring impulse was in 1957 by Nicholls et al.<sup>2</sup> who measured the specific impulse produced by a detonation tube using a ballistic pendulum technique. They measured the single-cycle specific impulse of acetylene- and hydrogen-oxygen mixtures and carried out some multi-cycle experiments using hydrogen-air; however, their experimental values are significantly lower than modern data.<sup>3-5</sup>

Zitoun and Desbordes<sup>6</sup> made an experimental determination of the impulse of a detonation tube using a stoichiometric ethylene-oxygen mixture by integrating the pressure history at the closed end of the tube. They performed their experiments for single-cycle and multi-cycle cases and observed a 30% decrease in the level of impulse for multi-cycle experiments. They attributed this impulse deficit to inadequate filling of the detonation tube. Zhdan et al.<sup>5</sup> measured the impulse generated by a stoichiometric acetylene-oxygen mixture in a short (0.125 or 0.25 m long) cylindrical detonation tube during single-cycle operation using a ballistic pendulum technique. The detonation tube was, in some cases, partially filled with air.

Schauer et al.<sup>3</sup> used a damped thrust stand to measure the impulse of a multi-cycle pulse detonation tube operating with hydrogen-air and more recently, hydrocarbon-air mixtures. Harris et al.<sup>7</sup> studied the effect of deflagration-to-detonation transition (DDT) distance on the impulse of a detonation tube using a ballistic pendulum technique with stoichiometric propane-oxygen mixtures diluted with nitrogen. They showed that there is no significant difference in impulse between directly initiated tests and DDT-initiated tests as long as DDT occurred in the tube and none of the combustible mixture was expelled from the tube prior to detonation.

The present study (preliminary results were given in Cooper et al.<sup>4</sup>) reports single-cycle impulse measurements for ethylene- and propane-oxygen-nitrogen mixtures in three tubes with different lengths, inner diameters, and internal obstacles using a ballistic pendulum arrangement with varying initial pressure and diluent amount. In a companion paper,<sup>1</sup> a simple model for impulse is developed and compared to both the present results and selected

results from the experiment studies quoted above. This analytical model<sup>1</sup> provides estimates for the impulse per unit volume and specific impulse of a single-cycle pulse detonation engine for a wide range of fuels (including aviation fuels) and initial conditions.

One of the original motivations of this experimental work was to provide a database useful for the validation of both numerical and analytic models. When our studies were initiated in 1999, there was substantial controversy over the impulse that could be obtained from an open-ended detonation tube. The present results, taken together with our simple model,<sup>1</sup> numerical simulations, and experiments of others (reviewed by Kailasanath<sup>8</sup>), demonstrate that at least for some fuels (ethylene), there is reasonable agreement of the impulse that can be obtained from a simple detonation tube.

The paper is organized as follows. First, we discuss the experimental details including the setup and impulse measurement technique with its associated uncertainty analysis. Second, we present experimental results on different DDT regimes followed by single-cycle impulse values for tubes containing spiral obstacles, single-cycle impulse values for tubes containing orifice or blockage plate obstacles, and single-cycle impulse values for tubes with extensions. Third, we discuss the implications of these results for pulse detonation engine technology.

## Experimental setup and procedure

The detonation tube of Figure 1 consisted of a constant area tube closed at one end by the thrust surface containing the ignition source and open at the other end but initially sealed with a 25  $\mu\text{m}$  thick Mylar diaphragm. The tube was hung from the ceiling by four steel wires in a ballistic pendulum arrangement shown schematically in Figure 2. Direct measurements were made of the impulse delivered by a DDT-initiated detonation or a flame by measuring the maximum horizontal displacement of the tube. The tube was evacuated to a pressure less than 13 Pa at the beginning of each experiment. Using the method of partial pressures, the individual gases comprising the initial mixture were added to the tube and subsequently mixed for 5 minutes with a circulation pump to ensure mixture homogeneity. A spark plug and associated discharge system with 30 mJ of stored energy was used to ignite the combustible mixture at the tube's thrust surface. Combustion products were free to expand out from the open end of the tube into a large ( $\simeq 50 \text{ m}^3$ ) blast-proof room. Pressure histories were measured at several locations along the tube length and at the thrust surface (Figure 3). Two of the tubes contained ionization gauges to measure the time-of-arrival of the flame or detonation front. The dimensions and diagnostic capabilities of the three detonation tubes tested are listed in Table 1.

The experimental variables included fuel type, initial pressure, diluent amount, and internal obstacles (Table 2). The internal obstacles included Shchelkin spirals, blockage plates,

and orifice plates, all with a blockage ratio of 0.43. The choice of blockage ratio, defined as the ratio of blocked area to the total area, was based on work by Lindstedt et al. who cite 0.44 as the optimal configuration.<sup>9</sup> No effort was made in this research to study the effect of blockage ratio on DDT or impulse.

The Shchelkin spirals were constructed of stainless steel tubing, with a diameter necessary to yield a blockage ratio of 0.43, coiled to fit inside the detonation tube (Figure 4). The spiral's pitch,  $p$ , refers to the axial distance between successive coils of the tubing. The spiral's length refers to the portion of the detonation tube length containing the spiral.

The blockage plate obstacles consisted of circular plates with an outer diameter smaller than the tube's inner diameter and of the size required to yield a blockage ratio of 0.43 (Figure 5). The blockage plates were suspended along the centerline of the detonation tube by a single threaded rod and spaced approximately one tube diameter apart. Their length refers to the length of the detonation tube containing the blockage plate obstacles.

The orifice plate obstacles consisted of a ring with an outer diameter equal to the inner diameter of the detonation tube and an inner diameter of the size necessary to yield a blockage ratio of 0.43 (Figure 6). The orifice plates were spaced approximately one tube diameter apart. Their length refers to the length of the detonation tube containing the orifice plate obstacles as measured from the thrust surface. The orifice plate obstacles that fill half of the detonation tube are referred to in the figures as "Half Orifice Plate" whereas the orifice plate obstacles that fill the entire tube length are referred to as "Orifice Plate" in the figures.

Three extensions attached to the open end of the 1.016 m length tube were tested and a description of each appears in a later section.

### **Impulse measurement and computation**

The impulse was determined by measuring the maximum horizontal deflection of the detonation tube, which is the oscillating mass of the ballistic pendulum. Each support wire was about 1.5 m in length so that the natural period of oscillation was about 2.45 s. During free oscillations, the maximum horizontal deflection occurs at a time equal to one-quarter of the period or 610 ms. The time over which the force is applied can be estimated<sup>1</sup> as  $10t_1$ , where  $t_1 = L/U_{CJ}$  is the time required for the detonation to propagate the length of the tube. For the longest tube tested, the time over which the force is applied is approximately 7.5 ms, which is significantly less than one-quarter of the oscillation period. Therefore, the classical analysis of an impulsively-created motion can be applied and the conservation of energy can be used to relate the maximum horizontal deflection to the initial velocity of the

pendulum. From elementary mechanics, the impulse is given by

$$I = m \sqrt{2gL_p \left( 1 - \sqrt{1 - \left( \frac{\Delta x}{L_p} \right)^2} \right)}. \quad (1)$$

This expression is exact given the assumptions discussed above and there are no limits on the values of  $\Delta x$ . Actual values of  $\Delta x$  observed in our experiments were between 50 and 300 mm. The impulse  $I$  measured in this fashion is referred to as the *ballistic* impulse, and is specific to a given tube size. Two measures of the impulse that are independent of tube size are the impulse per unit volume

$$I_V = I/V \quad (2)$$

and the specific impulse based on the total explosive mixture mass

$$I_{sp} = \frac{I}{g\rho_1 V}. \quad (3)$$

The impulse can also be calculated by placing a control volume around the detonation tube and considering the conservation of momentum. The conventional control volume used in rocket motor analysis is not suitable since the exit flow is unsteady and the required quantities (exit pressure and velocity) are unknown. It is more useful to place the control volume on the surface of the detonation tube (Figure 1) and write a force balance equation in the direction of the tube axis.

$$F = (P_{env} - P_{TS})A_{TS} + \sum_{obstacles} \int P \mathbf{n} \cdot \mathbf{x} dA + \int \tau dS + (P_{env} - P_{lip})A_{lip} \quad (4)$$

The first term on the right side of the equation is the force on the thrust surface, the second term is the drag (due to pressure differentials) over the obstacles, the third term is the viscous drag, and the last term represents the force over the tube wall thickness. The effect of heat transfer from the combustion products to the added surface area of the obstacles could also reduce the impulse due to a reduction of pressure internal to the detonation tube. We have not considered the role of heat transfer in the present investigation since our tubes are relatively short and the residence time is modest. We expect that heat transfer will become a significant issue for long tubes and/or tubes with exit restrictions that have long residence times for the hot products.

The impulse is obtained by integrating this force over a cycle,

$$I = \int F dt . \quad (5)$$

If all of the terms making up  $F$  can be computed or measured, the ballistic impulse and the impulse computed from this control volume integration should be identical. Previous studies<sup>6</sup> have used Equation 4 to analyze data from unobstructed tubes neglecting all but the first contribution to the force. This is a reasonable approximation when fast transition to detonation occurs; however, in the case of obstacles, the net contribution of the two drag terms may be substantial and using the first term alone can result<sup>10</sup> in overestimating the force and impulse by up to 50%. Since it is difficult to estimate or accurately measure all of the terms in Equation 4, direct measurement of the impulse is the only practical method for tubes with obstructions or other unusual features such as exit nozzles.

### Experimental uncertainties

An analysis was performed to quantify experimental uncertainties associated with the experimental setup and initial conditions using the standard method<sup>11</sup> for estimating error propagation. Generally, the variance  $\Delta I_V$  associated with the measured quantity  $I_V(x_1, \dots, x_n)$  can be estimated as

$$\Delta I_V = \sqrt{\left(\frac{\partial I_V}{\partial x_1}\right)^2 (\Delta x_1)^2 + \dots + \left(\frac{\partial I_V}{\partial x_n}\right)^2 (\Delta x_n)^2} .$$

Using the expression for ballistic impulse in Equation 1, the uncertainty in the direct experimental measurements of the impulse per unit volume can be quantified. The estimated uncertainties in the pendulum arm length, measured pendulum deflection, pendulum mass, and the tube volume are given in Table 3. From this analysis, the total uncertainty in the direct impulse measurements due to the experimental setup was calculated to be at most  $\pm 4\%$ .

Uncertainties in the initial conditions were also quantified. The measured leak rate was 50 Pa/min from an initial pressure of 13 Pa. The maximum time required to complete the experiment was 15 minutes which results in a worst-case air contamination of 810 Pa. A study to identify the mixture most affected by this leak rate found stoichiometric ethylene-oxygen at an initial pressure of 30 kPa and initial temperature of 295 K to be the most sensitive case. An error analysis was then performed for this mixture to find the maximum uncertainty in initial conditions for all experiments. The analytical model<sup>1</sup> can be used to express  $I_V$  as a function of  $U_{CJ}$ ,  $P_3$ , and  $c_3$ . The quantity  $\Delta U_{CJ}$  is the difference in the

Chapman-Jouguet velocity for a mixture containing an additional 810 Pa of air as a result of the leak and the ideal case. STANJAN<sup>12</sup> was used to calculate  $U_{CJ}$  in each case.  $\Delta P_3$  and  $\Delta c_3$  can then be found from differences in  $P_3$  and  $c_3$  for the two mixtures, where  $P_3$  and  $c_3$  are given by the relationships below, which are derived by using the method of characteristics to relate flow properties on either side of the Taylor wave,<sup>1</sup>

$$\frac{P_3}{P_2} = \left(\frac{c_3}{c_2}\right)^{\frac{2\gamma}{\gamma-1}} = \left(\frac{\gamma+1}{2} - \frac{\gamma-1}{2} \frac{U_{CJ}}{c_2}\right)^{\frac{2\gamma}{\gamma-1}}. \quad (6)$$

Table 4 lists the calculated maximum changes in the flow parameters due to the leak rate. Also shown are the largest possible contributions due to uncertainty in the initial pressure because of gauge precision ( $\pm 0.1$  kPa) and due to uncertainty in the initial temperature (295-298 K). All uncertainties shown are calculated for comparison with the same ideal case specified above.

Combining the results in Table 4, the uncertainty in the impulse measurement due to the initial conditions is found to contribute at most  $\pm 2.3\%$ , resulting in an overall maximum uncertainty of  $\pm 6.3\%$  in ballistic measurements of the impulse.

Experimental repeatability was also considered. For experiments in which fast transition to detonation occurred, the impulse was repeatable to within  $\pm 0.7\%$ . In cases where late DDT or fast flames were observed, the impulse in repeat experiments varied by as much as  $\pm 17\%$  due to the turbulent nature of the flow during the initiation process. Additional experiments were conducted to verify that no out-of-plane motion existed during the initial pendulum swing.

The mass of the diaphragm was 0.27 g. For comparison, the mass of the ethylene-air mixture at 50 kPa (one of the lighter mixtures) is 3.3 g. Since the mass of the diaphragm is 8% of the total explosive mixture mass, we expect that in the worst case, this would have a tamping effect equivalent to adding an inert gas-filled extension that is 8% of the original tube length. We estimate<sup>13</sup> that this would have the effect of slightly (1-2%) increasing the impulse over the ideal (zero mass diaphragm) case. However, since the diaphragm is located at the end of the tube, the movement of the diaphragm away from the tube exit following the arrival of the detonation is expected to rapidly diminish the tamping effect.

Uncertainty in the DDT times was determined using the distance between two successive ionization probes and the Chapman-Jouguet velocity calculated with STANJAN<sup>12</sup> for each of the initial mixtures. In the experiments, transition to detonation was marked by a measured wave velocity greater than the calculated Chapman-Jouguet velocity followed by a relaxation to the expected detonation velocity. Thus, dividing the distance between two successive



ionization gauges by the calculated detonation velocity (instead of the overdriven detonation velocity observed at the transition) results in an upper bound on the uncertainty of  $\pm 46.4 \mu\text{s}$ .

## Experimental Results

### Detonation initiation regimes

As stated in the experimental setup, all mixtures were ignited by a spark with a discharge energy (30 mJ) less than the critical energy required for direct initiation of a detonation (approximately 283 kJ for propane-air mixtures<sup>14</sup> and approximately 56 kJ for ethylene-air mixtures<sup>14</sup> at atmospheric conditions). Thus, detonations were obtained only by transition from an initial deflagration. The presence of a deflagration is denoted by a gradual rise in the pressure histories as the unburned gas ahead of the flame is compressed due to the expansion of the burned gases behind the flame. If the correct conditions exist, this initial deflagration can transition to a detonation wave. Otherwise, transition will not occur and the deflagration wave will travel the entire length of the tube. An abrupt pressure jump ( $\Delta P > 2$  MPa for hydrocarbon fuels) is indicative of this transition which can be quantified in terms of both the DDT time (from spark firing) and DDT distance (axial distance from ignition source location) required for the event to occur.

Through multiple experiments with varying mixtures and internal obstacles, pressure histories and ionization gauges data were used to identify several combustion regimes including the DDT process. The pressure transducers were protected by a layer of thermally-insulating vacuum grease. While this delays the onset of heating of the gauge surface, our experience is that eventually thermal artifacts will be produced in the signal. Although we have not quantified this for the present experiments, the pressure signals are reproducible and physically reasonable.

These different combustion regimes are categorized as fast transition to detonation (Figure 7), slow transition to detonation (Figure 8), fast flames (Figure 9), and slow flames (Figure 10). Figure 7 illustrates the case of a fast transition to detonation, defined by an abrupt pressure increase before the first pressure transducer along the tube axis and the low DDT time. Figure 8 illustrates a slow transition to detonation case. An accelerating flame produces a gradual increase in pressure with time at the first and second pressure transducers, and transition to a detonation occurs between the second and third pressure transducers. In this case, the transition occurs late in the tube resulting in a longer DDT time. Figure 9 illustrates the case of a fast flame. The flame speed is fast enough to create significant compression waves but transition to detonation does not occur. Figure 10 illustrates the case of a slow flame. The flame speed is low and only smooth pressure waves of low amplitude ( $< 0.5$  MPa) are generated.

For cases when transition to detonation did occur, the DDT time was determined by measuring the combustion wave velocity and comparing this to the Chapman-Jouguet detonation velocity,  $U_{CJ}$ . The combustion wave velocity was estimated as the ratio of the distance between ionization probes to the time it took the reaction zone to pass from one ionization probe to the next. Transition is said to have occurred when this average combustion wave velocity is equal to or greater than the Chapman-Jouguet detonation velocity. The relative ability of the mixture to transition to detonation can be related to<sup>15,16</sup> mixture properties such as the detonation cell size, expansion ratio, and deflagration speed. Necessary conditions for DDT are that the cell width be smaller than a specified fraction of the tube or obstacle dimensions, the expansion ratio (ratio of burned to unburned gas volume) must be larger than a minimum value, and that the deflagration speed exceeds a minimum threshold. For cases of a straight tube, transition to detonation is possible only if the detonation cell width is smaller than the tube diameter (unobstructed tube) or smaller than the obstacles' aperture (obstructed tube).

Figures 11 and 12 plot the DDT time for ethylene-oxygen-nitrogen mixtures in the 1.016 m long tube as a function of the initial pressure and diluent amount. Transition to detonation occurred in an unobstructed tube for mixtures at an initial pressure between 30 and 100 kPa and for mixtures up to 30% nitrogen. Since cell size increases with decreasing initial pressure and increasing dilution, the largest cell size was about 0.5 mm<sup>14</sup> corresponding to ethylene-oxygen at 30 kPa and about 0.6 mm<sup>14</sup> corresponding to ethylene-oxygen-nitrogen at 30% dilution. For these two cases, the inclusion of obstacles reduced the DDT time by an average of 65%. Additionally, the obstacles allowed DDT to occur in mixtures composed of up to 60% nitrogen (Figure 12), corresponding to an approximate cell size of 10 mm,<sup>14</sup> as compared with DDT being achieved only up to 30% nitrogen in a tube with no obstacles. Thus, the presence of obstacles enabled mixtures with more diluent (less sensitive mixtures with a larger cell size) to transition to detonation, but there are limits to obstacle effectiveness. This is illustrated by the ethylene-air (74% nitrogen dilution) mixture with an approximate cell size of 29 mm<sup>14</sup> which did not transition to a detonation. Wintenberger et al.<sup>1</sup> have used the ideas of Dorofeev et al.<sup>15</sup> to estimate limits for DDT in obstructed tubes that are consistent with our observations.

### Impulse measurements

The following two sections present single-cycle impulse measurements with internal obstacles. To facilitate comparison between the different tube sizes, the results are given in terms of impulse normalized by the tube volume,  $I_V$ , as well as the mixture-based specific impulse,  $I_{sp}$ . The figures also show predicted impulse values from a model<sup>1</sup> that is based on analysis

of the gas dynamic processes in the tube. The model impulse values are generally within 15% of the experimental impulse values over the range of pressures and diluent amounts studied. Wintenberger et al.<sup>1</sup> provide additional discussion of differences between the experimental and model impulse values. As seen in both the measured and model data,<sup>1</sup> the impulse per unit volume increases linearly with increasing initial pressure while the specific impulse tends to a constant value. The measured and model data<sup>1</sup> also show that both the impulse per unit volume and specific impulse decrease with increasing nitrogen dilution. This is due to the reduced amount of fuel present in a given volume of mixture with increasing amounts of dilution, which reduces the total energy released during combustion.

### *Experiments with spiral obstacles*

Direct impulse measurements for propane-oxygen-nitrogen mixtures were made in two tubes of lengths of 0.609 m and 1.5 m with different Shchelkin spiral configurations. Figure 13 shows impulse as a function of initial pressure for both tubes and Figure 14 shows impulse as a function of diluent amount for the 0.609 m tube only.

From Figure 13, it can be seen that the obstacles with a smaller pitch cause a greater reduction in impulse than those with a larger pitch. We attribute this loss in impulse as being due to a greater form drag associated with the flow around the obstacles as the spiral pitch decreases. At 100 kPa, a 5% reduction in the distance between successive coils causes a 13% reduction in impulse if the spirals extend over the entire tube length.

If DDT does not occur, the impulse is reduced (Figure 14). DDT limits were discussed in the previous section, but now the effect of late or no DDT on impulse can be investigated. As the mixture sensitivity decreases with increasing dilution, it becomes progressively more difficult to initiate a detonation within the tube. For large amounts of diluent, DDT does not occur within the tube and only deflagrations are observed (Figures 9 and 10). Deflagrations propagate down the tube at a relatively slower flame speed compressing the unburned gas ahead of the flame. This unburned gas compression is sufficient to rupture the thin diaphragm causing a considerable part of the mixture to be ejected outside the tube. Observations made by Jones and Thomas<sup>17</sup> clearly demonstrate the gas motion and compression waves ahead of the flame. The mixture ejected from the tube does not contribute to the impulse due to its unconfined burning. The effect of this mixture spillage due to no DDT can be seen in the cases with greater than 70% diluent where a 30-50% reduction in impulse is observed. The onset of a detonation wave can mitigate this effect due to its higher propagation speed. If DDT occurs early enough in the process, the detonation can overtake the compression waves created by the deflagration before they reach the diaphragm. The loss associated with this phenomenon is expected to become significant when DDT occurs in the last quarter of the

tube, so that the detonation does not have time to catch up with the deflagration compression waves. Cases of late or no DDT illustrate the importance of more sophisticated initiation methods for less sensitive fuels, such as storable liquid hydrocarbons (Jet A, JP-8, JP-5 or JP-10) with cell widths similar to propane. Experiments with more sensitive ethylene-oxygen-nitrogen mixtures show that using obstacles to induce DDT within the tube can be effective.

### *Experiments with orifice and blockage plate obstacles*

Impulse measurements for ethylene-oxygen mixtures in the 1.016 m long tube appear in Figure 15 as a function of initial pressure and Figure 16 as a function of nitrogen dilution. Also shown are the analytical model predictions.<sup>1</sup> Without obstacles, detonation cannot be achieved in this tube for nitrogen dilutions of 40% or greater. A dramatic drop in measured impulse results for these mixtures (Figure 16). The addition of obstacles enabled DDT to occur in mixtures up to 60% nitrogen dilution. Beyond this point, the cell width is sufficiently large that transition to detonation occurs only in the latter portion of the tube and not all of the mixture burns within the tube.

Although obstacles can induce DDT in less sensitive mixtures and significantly increase the impulse, the obstacle drag can decrease the impulse by an average of 25% from the value measured without obstacles when fast transition to a detonation occurs (Figure 15). This impulse loss is due to additional drag from the obstacles and added heat transfer to the obstacles reducing the energy available for conversion into thrust.

## **Effect of extensions**

Proposed concepts for pulse detonation engines have often included the addition of different kinds of extensions, including nozzles, to the basic straight detonation tube. In part, this is motivated by the effectiveness of converging-diverging nozzles in conventional rocket motors. The effectiveness of a converging-diverging nozzle is based on the steady flow conversion of the thermal to kinetic energy. However, the pulse detonation engine is an unsteady device that relies on waves to convert the thermal energy into kinetic energy. It is not obvious how a nozzle would affect performance since the diffraction of the detonation wave through a nozzle is a complex process that involves significant losses.

We have approached this problem experimentally by examining the effect of various exit treatments on the measured impulse. Previous experiments by Zhdan et al.<sup>5</sup> with straight cylindrical extensions indicate that the mixture-based specific impulse will increase as the ratio of the overall tube length,  $L_t$ , to the tube length filled with combustible gases,  $L$ , increases. Note that the mass of air in the extension volume is not included in the mixture mass used to compute the specific impulse. In our tests, as in Zhdan et al.,<sup>5</sup> a thin diaphragm

separates the tube length filled with the combustible mixture from the extension, which was filled with air at atmospheric conditions. This simulates the condition of having a single tube only partially filled with explosive mixture.

### **Extensions tested**

Three different extensions were tested on the detonation tube with a length of 1.016 m in a ballistic pendulum arrangement to determine their effect on the impulse. Each extension modified the total tube length,  $L_t$ , while the charge length,  $L$ , remained constant.

The first extension was a flat plate ( $L_t/L = 1$ ) or flange with an outer diameter of 0.381 m that extended radially in the direction perpendicular to the tube's exhaust flow. A hole located in the center of the plate matched the tube's inner diameter, thus increasing the apparent wall thickness at the exhaust end from 0.0127 m to 0.1524 m. The purpose of this flange was to see if the pressure behind the diffracting shock wave would contribute significantly to the specific impulse. In effect, this examines the role of the last term (wall thickness) of Equation 4 in the momentum control volume analysis. The second extension was a straight cylinder ( $L_t/L = 1.6$ ) with a length of 0.609 m. This extension simulated a partial fill case. The third extension was a diverging conical nozzle ( $L_t/L = 1.3$ ) with a half angle of eight degrees and a length of 0.3 m.

### **Impulse measurements**

The flat plate and straight extension were tested with ethylene-oxygen-nitrogen mixtures on a tube that did not contain internal obstacles (Figure 17).

The flat plate extension yielded a maximum specific impulse increase of 5% at 0% nitrogen dilution which is within our uncertainty in measured impulse. This effect can be understood by recognizing that the flat plate or flange extension has a minimal effect on the impulse since the shock Mach number decays very quickly as the shock diffracts out from the open end. The amount of impulse contributed by the pressure of the decaying shock is relatively small compared to that obtained from the pressure of the detonation products on the thrust surface at the closed end of the tube. In addition, the rate of pressure decrease at the exit is relatively unaffected by the flange so that the rate of pressure decay at the thrust surface is very similar with and without the flat plate. At 40% nitrogen dilution, DDT did not occur and the flat plate extension decreased the impulse by 7%. This percentage decrease is within the experimental uncertainty for cases with late or no DDT, preventing any conclusion about the plate's performance for this test case.

The straight extension increased the measured specific impulse by 18% at 0% nitrogen dilution, whereas a 230% increase in the specific impulse was observed at 40% nitrogen dilution. This large increase in the specific impulse occurred since the additional tube length

enabled DDT to occur in the extension's confined volume.

To better isolate the effect of the extensions over the range of diluent percentages tested, cases of late or no DDT were eliminated by the addition of the "Half orifice plate" obstacles (Figure 6). Both the straight extension and diverging nozzles were tested as a function of diluent amount (Figure 18). The flat plate extension was not retested due to its small effect on the measured impulse shown previously. The straight extension attached to a tube with internal obstacles increased the specific impulse by an average of 13%. As shown above, the straight extension attached to a tube without internal obstacles increased the impulse by 18%. This 5% reduction in impulse is due to drag and heat transfer losses induced by the obstacles. The diverging nozzle had a minor effect, increasing the specific impulse by an average of 1%, which is within the experimental uncertainty.

The straight extension was more effective than the diverging nozzle in increasing impulse (Figure 18). One explanation<sup>5,18</sup> of this effect is that the additional length of the straight extension as compared with the diverging extension delays the arrival of the expansion wave from the tube exit, effectively increasing the pressure relaxation time and the impulse. Standard gas dynamics considerations indicate that two reflected waves will be created when an extension filled with inert gas is added to a detonation tube. The first wave is due to the interaction of the detonation with the mixture-air interface and is much weaker than the wave created by the shock or detonation diffraction at the tube exit. Additionally, the continuous area change of the diverging nozzle creates expansion waves that propagate back to the thrust surface resulting in a gradual but continuous decrease in pressure that starts as soon as the detonation reaches the entrance to the diverging nozzle. Another way to interpret these impulse results with added extensions is that the added inert gas provides additional tamping<sup>13</sup> of the explosion which will increase the momentum transfer from the detonation products to the tube.

## Summary and Conclusion

Single-cycle impulse measurements were made for deflagrations and detonations initiated with a 30 mJ spark in three tubes of different lengths and inner diameters. A ballistic pendulum arrangement was used and the measured impulse values were compared to those obtained from an analytical model.<sup>1</sup> The measured impulse values were estimated to have an uncertainty of  $\pm 6.3\%$  in cases where DDT occurred sufficiently early within the tube. By studying the pressure histories measured at several locations in the tube, four internal flow regimes were identified. Internal obstacles, with a constant blockage ratio of 0.43, were used to reduce DDT times and initiate detonations in insensitive mixtures such as those with a high diluent amount. Times to transition were measured with ionization probes. The

internal obstacles were found to reduce DDT times for insensitive mixtures and even enable highly insensitive mixtures (up to 60% dilution in ethylene-oxygen mixtures) to transition. However, the effectiveness of the obstacles is limited since detonations could not be obtained in ethylene-air (75% dilution) in the 1.016 m tube. It was determined that those regimes in which slow or no transition to detonation occurred resulted in impulse values 30-50% lower than model<sup>1</sup> predictions. For cases of fast transition to detonation, the inclusion of obstacles decreased the measured impulse by an average of 25% as compared with the measured impulse for a tube without internal obstacles.

The effect of different exit arrangements was studied by using three different types of extensions. A relationship between the overall length-to-charge length ( $L_t/L$ ) ratio and impulse was observed. The straight extension, with a  $L_t/L$  ratio of 1.6, resulted in the greatest increase in impulse of 18% at 0% dilution and no internal obstacles. This increase in impulse is due to the increase in momentum transfer to the tube due to the additional mass contained in the extension.

The results of this experimental work have several significant implications for pulse detonation engine technology. The use of internal obstacles may be effective in initiating detonations in highly insensitive mixtures of larger cell widths such as all the storable liquid hydrocarbon fuels. However, because there are limits to obstacle effectiveness, their use will have to be optimized for a given mixture and application. The use of extensions may also be beneficial in augmenting the specific impulse obtainable from a given fuel-oxidizer mass. However, the maximum impulse is always obtained by filling the available tube volume entirely with the combustible mixture. Additional studies in progress are required to quantify the effect on impulse that could be obtained with diverging and converging-diverging nozzles.

## Acknowledgment

This work was supported by the Office of Naval Research Multidisciplinary University Research Initiative *Multidisciplinary Study of Pulse Detonation Engine* (grant 00014-99-1-0744, sub-contract 1686-ONR-0744), and General Electric contract GE-PO A02 81655 under DABT-63-0-0001.

## References

<sup>1</sup>Wintenberger, E., Austin, J., Cooper, M., Jackson, S., and Shepherd, J. E., "An Analytical Model for the Impulse of a Single-Cycle Pulse Detonation Engine," 37th AIAA/ASME/SAE/ASEE Joint Propulsion Conference, July 8–11, 2001, Salt Lake City, UT, AIAA 2001-3811.

<sup>2</sup>Nicholls, J. A., Wilkinson, H. R., and Morrison, R. B., "Intermittent Detonation as a Thrust-Producing Mechanism," *Jet Propulsion*, Vol. 27, No. 5, 1957.

<sup>3</sup>Schauer, F., Stutrud, J., and Bradley, R., “Detonation Initiation Studies and Performance Results for Pulsed Detonation Engines,” 39th AIAA Aerospace Sciences Meeting and Exhibit, January 8–11, 2001, Reno, NV, AIAA 2001-1129.

<sup>4</sup>Cooper, M., Jackson, S., Austin, J., Wintenberger, E., and Shepherd, J. E., “Direct experimental impulse measurements for deflagrations and detonations,” 37th AIAA/ASME/SAE/ASEE Joint Propulsion Conference, July 8–11, 2001, Salt Lake City, UT, AIAA 2001-3812.

<sup>5</sup>Zhdan, S. A., Mitrofanov, V. V., and Sychev, A. I., “Reactive Impulse from the Explosion of a Gas Mixture in a Semi-infinite Space,” *Combustion, Explosion and Shock Waves*, Vol. 30, No. 5, 1994, pp. 657–663.

<sup>6</sup>Zitoun, R. and Desbordes, D., “Propulsive Performances of Pulsed Detonations,” *Comb. Sci. Tech.*, Vol. 144, 1999, pp. 93–114.

<sup>7</sup>Harris, P. G., Farinaccio, R., and Stowe, R. A., “The Effect of DDT Distance on Impulse in a Detonation Tube,” 37th AIAA/ASME/SAE/ASEE Joint Propulsion Conference and Exhibit, July 8–11, 2001, Salt Lake City, UT, AIAA 2001-3467.

<sup>8</sup>Kailasanath, K., “Recent Developments in the Research on Pulse Detonation Engines,” 40th AIAA Aerospace Sciences Meeting and Exhibit, January 14–17, 2002, Reno, NV, AIAA 2002-0470.

<sup>9</sup>Lindstedt, R. P. and Michels, H. J., “Deflagration to Detonation Transitions and Strong Deflagrations in Alkane and Alkene Air Mixtures,” *Combust. Flame*, Vol. 76, 1989, pp. 169–181.

<sup>10</sup>Cooper, M., Jackson, S., and Shepherd, J. E., “Effect of Deflagration-to-Detonation Transition on Pulse Detonation Engine Impulse,” GALCIT Report FM00-3, Graduate Aeronautical Laboratories, California Institute of Technology, Pasadena, CA 91125, 2000.

<sup>11</sup>Bevington, P. R., *Data Reduction and Error Analysis in the Physical Sciences*, McGraw-Hill, 1969.

<sup>12</sup>Reynolds, W. C., “The Element Potential Method for Chemical Equilibrium Analysis: Implementation in the Interactive Program STANJAN, Version 3,” Tech. rep., Dept. of Mechanical Engineering, Stanford University, Stanford, CA, January 1986.

<sup>13</sup>Kennedy, J. E., “The Gurney Model of Explosive Output for Driving Metal,” *Explosive Effects and Applications*, edited by J. A. Zuker and W. P. Walters, chap. 7, Springer, New York, 1998, pp. 221–257.

<sup>14</sup>Shepherd, J. E. and Kaneshige, M., “Detonation Database,” Tech. Rep. GALCIT Report FM97-8, California Institute of Technology, 1997, Revised 2001 - see [www.galcit.caltech.edu/detn\\_db/html](http://www.galcit.caltech.edu/detn_db/html) for the most recent version.



<sup>15</sup>Dorofeev, S., Sidorov, V. P., Kuznetsov, M. S., Matsukov, I. D., and Alekseev, V. I., “Effect of scale on the onset of detonations,” *Shock Waves*, Vol. 10, 2000.

<sup>16</sup>Dorofeev, S., Kuznetsov, M., Alekseev, V., Efimenko, A., and Breitung, W., “Evaluation of limits for effective flame acceleration in hydrogen mixtures,” *Journal of Loss Prevention in the Process Industries*, Vol. 14, No. 6, 2001, pp. 583–589.

<sup>17</sup>Jones, S. A. S. and Thomas, G. O., “Pressure Hot-Wire and Laser Doppler Anemometer Studies of Flame Acceleration in Long Tubes,” *Combust. Flame*, Vol. 87, 1991, pp. 21–32.

<sup>18</sup>Chiping, L., Kailasanath, K., and Patnaik, G., “A Numerical Study of Flow Field Evolution in a Pulsed Detonation Engine,” 38th AIAA Aerospace Sciences Meeting and Exhibit, January 10–13, 2000, Reno, NV, AIAA 2000–0314.

## List of Tables

1	Dimensions and diagnostic capabilities of tested detonation tubes. . . . .	19
2	Experimental variables of tested detonation tubes. . . . .	20
3	Uncertainties used in determining the error for experimentally measured impulse. . . . .	21
4	Variations in flow parameters resulting from uncertainty in initial conditions due to error in dilution (leak rate), initial pressure, and initial temperature as described in the text. The mixture chosen is stoichiometric C <sub>2</sub> H <sub>4</sub> -O <sub>2</sub> at an initial pressure of 30 kPa, which corresponds to the worst case of all the mixtures considered in experiments. The percentage error in $I_V$ is based on the model predicted impulse. <sup>1</sup> . . . . .	22

Length [m]	Diameter [mm]	Pressure Transducers	Ion Gauges
0.609	76.2	3 and 1 at Thrust Surface	4
1.016	76.2	3 and 1 at Thrust Surface	10
1.5	38.0	3	0

**Table 1: Dimensions and diagnostic capabilities of tested detonation tubes.**

Length	Fuels Tested	Pressures [kPa]	Nitrogen [%]	Internal Obstacles
0.609 m	C <sub>3</sub> H <sub>8</sub>	50 - 100	0 - air	Spiral with length = 0.609 m, p = 28 mm Spiral with length = 0.609 m, p = 51 mm
1.016 m	C <sub>2</sub> H <sub>4</sub>	30 - 100	0 - air	No Internal Obstacles Blockage Plate with length = 1.016 m Orifice Plate with length = 1.016 m Half Orifice Plate with length = 0.508 m
1.5 m	C <sub>3</sub> H <sub>8</sub>	50 - 100	0 - air	Spiral with length = 0.305 m, p = 11 mm

**Table 2: Experimental variables of tested detonation tubes.**

Quantity	Range of values	Uncertainty
$L_p$	1.4-1.55 m	$\pm 0.0016$ m
$\Delta x$	2-292 mm	$\pm 0.5$ mm
$m$	12.808-55.483 kg	$\pm 0.001$ kg
$V$	$1.14-4.58 \times 10^{-3}$ m <sup>3</sup>	$\pm 4.5 \times 10^{-8}$ m <sup>3</sup>

**Table 3:** Uncertainties used in determining the error for experimentally measured impulse.

	Ideal	Dilution	Pressure	Temperature
$P_1$ (kPa)	30.0	30.0	30.1	30.0
$T_1$ (K)	295	295	295	298
$U_{CJ}$ (m/s)	2317.9	2301.3	2307.5	2317.3
$P_2$ (kPa)	970.2	955.2	965.4	960.0
$c_2$ (m/s)	1249.	1240.	1243.	1249.
$\gamma$	1.23	1.23	1.23	1.23
$P_3$ (kPa)	318.5	314.8	317.2	315.3
$c_3$ (m/s)	1123.	1117.	1119.	1123.
$\Delta U_{CJ}$ (m/s)	-	16.6	10.4	0.6
$\Delta P_3$ (Pa)	-	3620	1242	3185
$\Delta c_3$ (m/s)	-	6.2	4.6	0.040
$\Delta I_V$	-	1.7%	0.6%	1.5%

**Table 4:** Variations in flow parameters resulting from uncertainty in initial conditions due to error in dilution (leak rate), initial pressure, and initial temperature as described in the text. The mixture chosen is stoichiometric  $C_2H_4-O_2$  at an initial pressure of 30 kPa, which corresponds to the worst case of all the mixtures considered in experiments. The percentage error in  $I_V$  is based on the model predicted impulse.<sup>1</sup>

## List of Figures

1	Pulse detonation engine control volume. . . . .	24
2	Ballistic pendulum arrangement for direct impulse measurement. . . . .	25
3	Sample pressure trace of stoichiometric $C_2H_4-O_2$ at 100 kPa initial pressure recorded at the thrust surface. . . . .	26
4	Arrangement of spiral obstacles inside detonation tube. . . . .	27
5	Blockage Plate Obstacles: a) Dimensions of blockage plates in millimeters. b) Arrangement of blockage plates inside detonation tube. . . . .	28
6	Orifice Plate Obstacles: a) Dimensions of orifice plates in millimeters. b) Arrangement of orifice plates inside detonation tube for the “Orifice Plate” configuration. c) Arrangement of orifice plates inside detonation tube for the “Half Orifice Plate” configuration. . . . .	29
7	Pressure history recorded for a stoichiometric $C_3H_8-O_2$ mixture at 100 kPa initial pressure in the 0.609 m long tube illustrating the fast transition to detonation case. . . . .	30
8	Pressure history recorded for a stoichiometric $C_3H_8-O_2-N_2$ mixture with $\beta = 1.5$ at 100 kPa initial pressure in the 0.609 m long tube illustrating the slow transition to detonation case. . . . .	31
9	Pressure history recorded for a stoichiometric $C_3H_8-O_2-N_2$ mixture with $\beta = 3$ at 100 kPa initial pressure in the 0.609 m long tube illustrating the fast flame case. . . . .	32
10	Pressure history recorded for a stoichiometric $C_3H_8$ -air mixture at 100 kPa initial pressure in the 0.609 m long tube illustrating the slow flame case. . . . .	33
11	Measured DDT time for stoichiometric $C_2H_4-O_2$ mixtures with varying initial pressure for three obstacle configurations in the 1.016 m long tube. . . . .	34
12	Measured DDT time for stoichiometric $C_2H_4-O_2$ mixtures with varying nitrogen dilution at 100 kPa initial pressure for three obstacle configurations in the 1.016 m long tube. . . . .	35
13	Impulse measurements for stoichiometric $C_3H_8-O_2$ mixtures with varying initial pressure in the 1.5 m and 0.609 m long tubes. . . . .	36
14	Impulse measurements for stoichiometric $C_3H_8-O_2$ mixtures with varying nitrogen dilution at 100 kPa initial pressure in the 0.609 m long tube. . . . .	37
15	Impulse measurements for stoichiometric $C_2H_4-O_2$ mixtures with varying initial pressure in the 1.016 m long tube. . . . .	38
16	Impulse measurements for stoichiometric $C_2H_4-O_2$ mixtures with varying nitrogen dilution at 100 kPa initial pressure in the 1.016 m long tube. . . . .	39
17	Specific impulse for stoichiometric $C_2H_4-O_2$ mixtures at 100 kPa initial pressure with varying diluent and no internal obstacles. . . . .	40
18	Specific impulse for stoichiometric $C_2H_4-O_2$ mixtures at 100 kPa initial pressure with varying diluent and “Half Orifice Plate” internal obstacles. . . . .	41

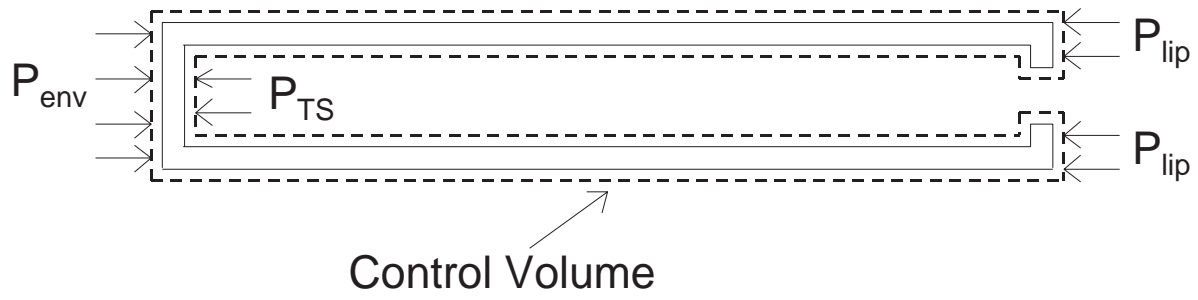


Figure 1: Cooper et al.



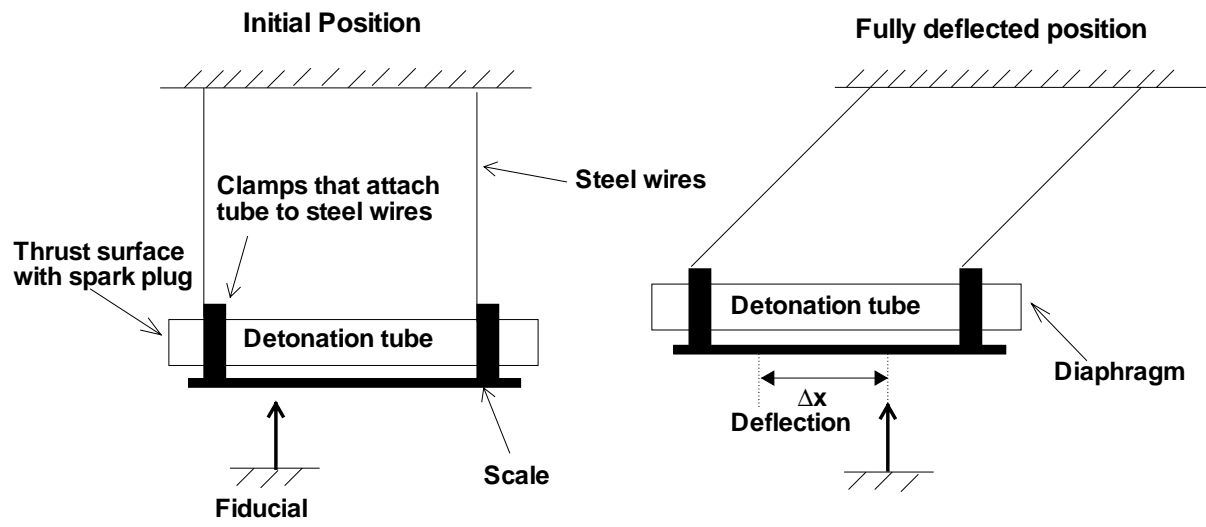


Figure 2: Cooper et al.

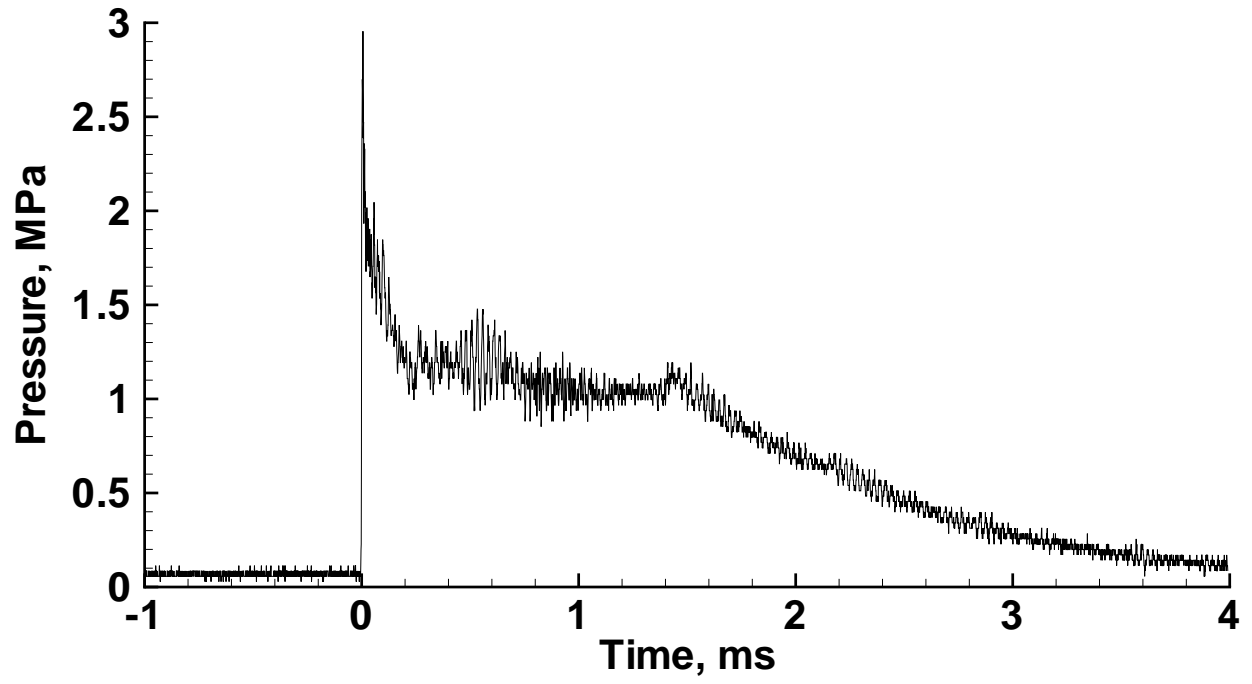


Figure 3: Cooper et al.

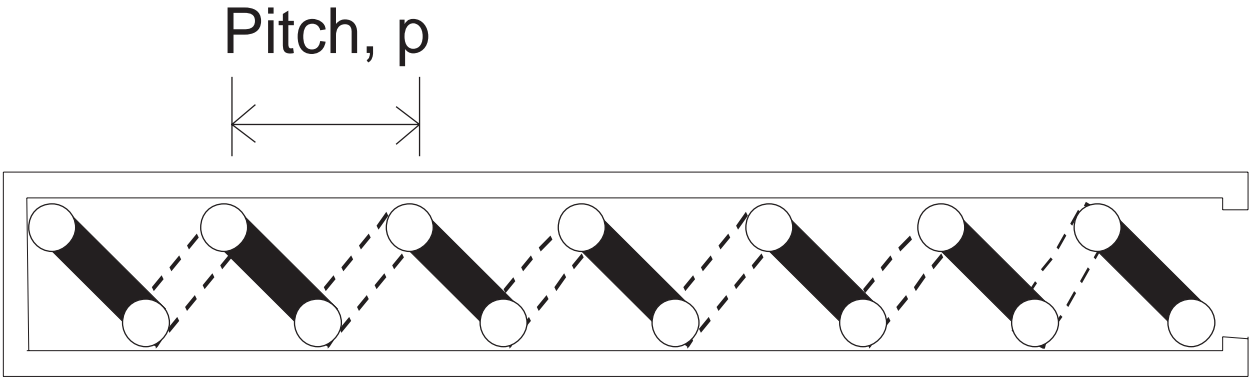
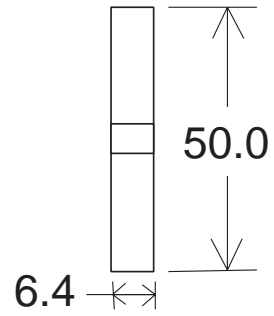
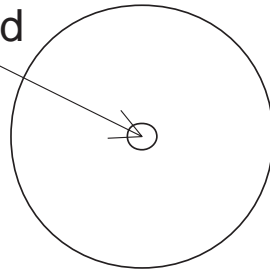


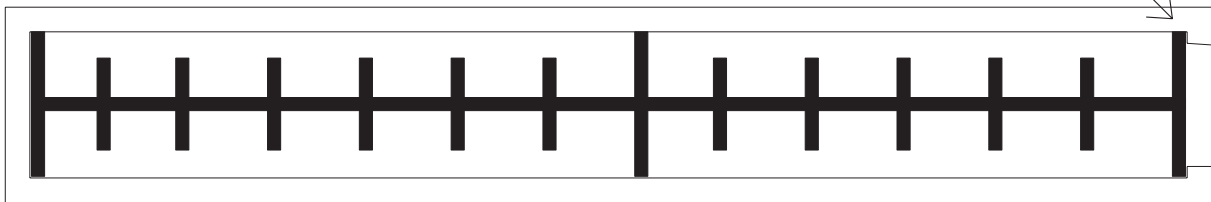
Figure 4: Cooper et al.

Clearance hole for  
6.4 mm threaded  
rod



(a)

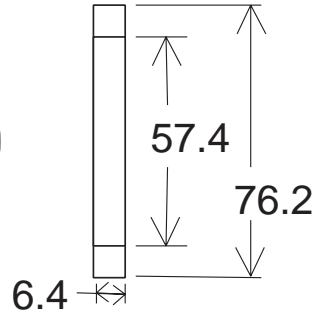
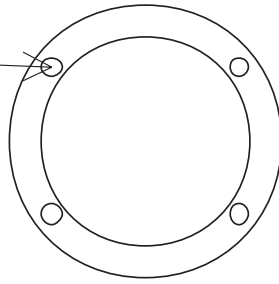
Supports (3 places)



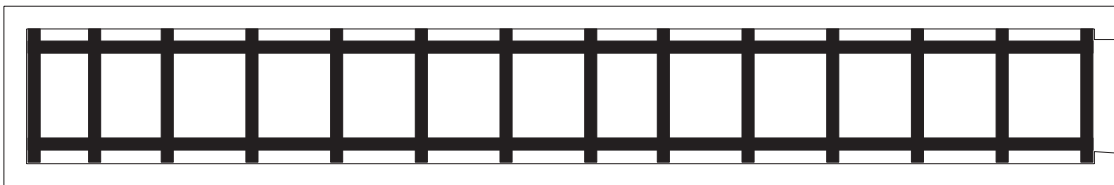
(b)

Figure 5: Cooper et al.

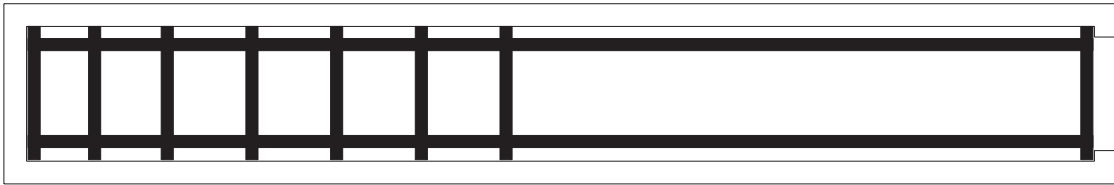
Clearance hole for  
6.4 mm threaded  
rod (4 places)



(a)



(b)



(c)

Figure 6: Cooper et al.

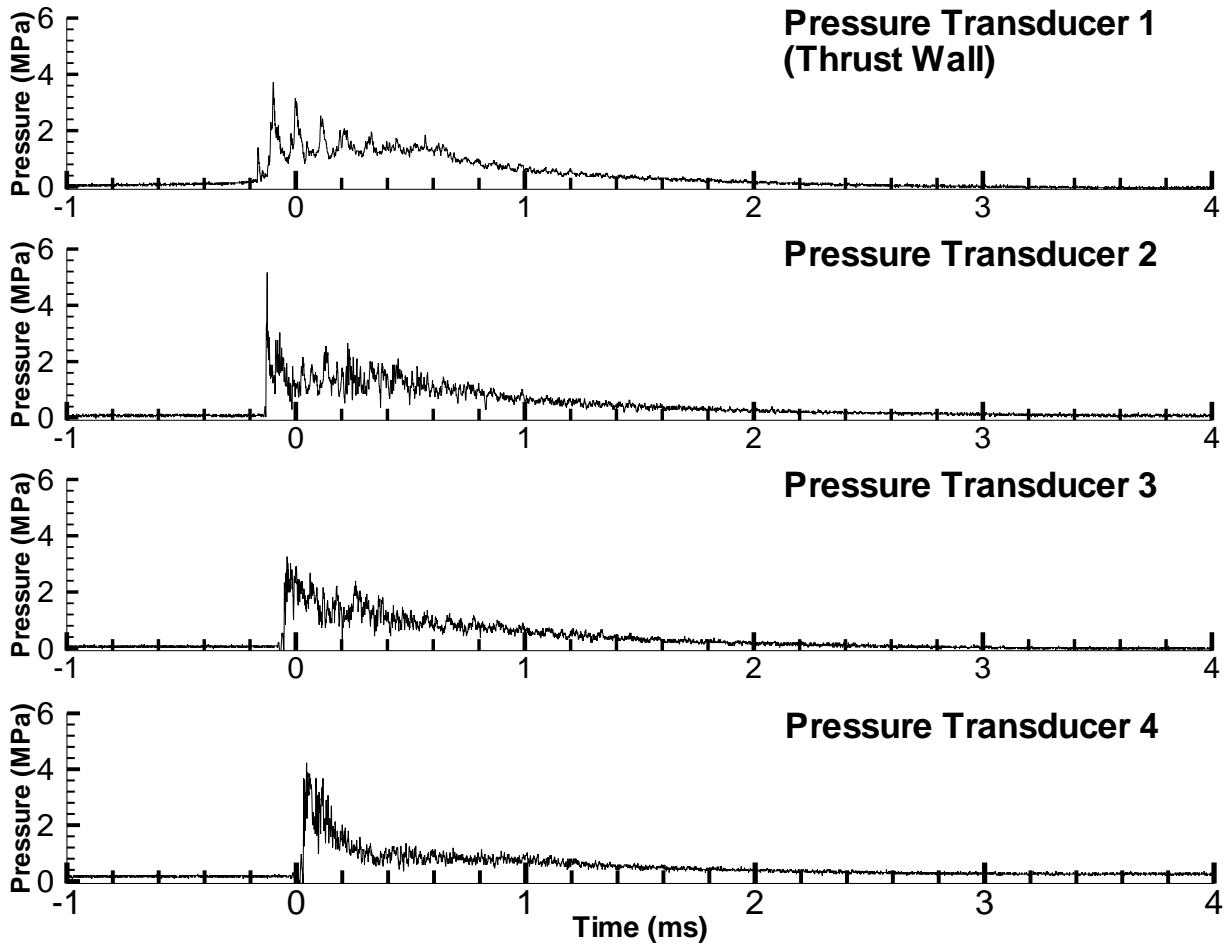


Figure 7: Cooper et al.

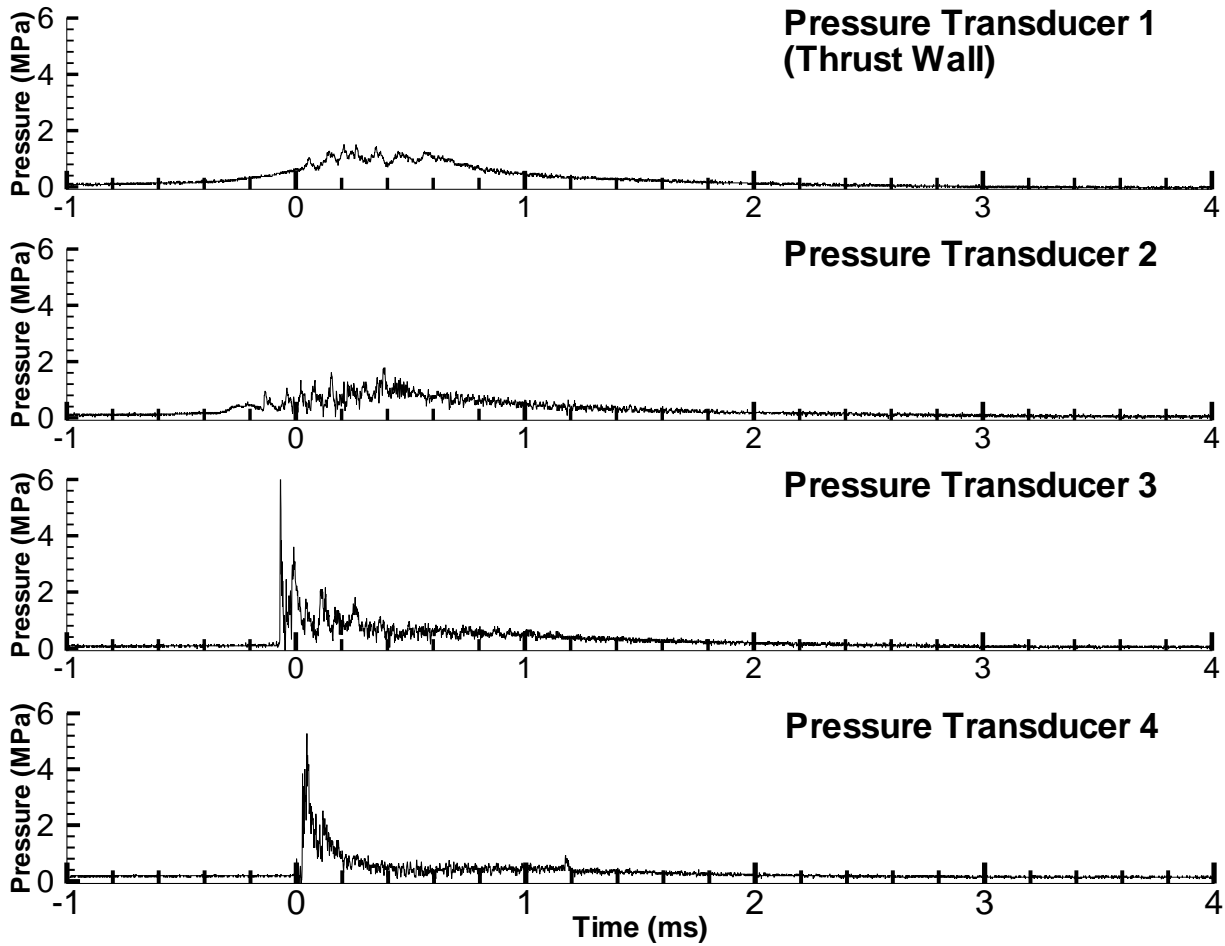


Figure 8: Cooper et al.

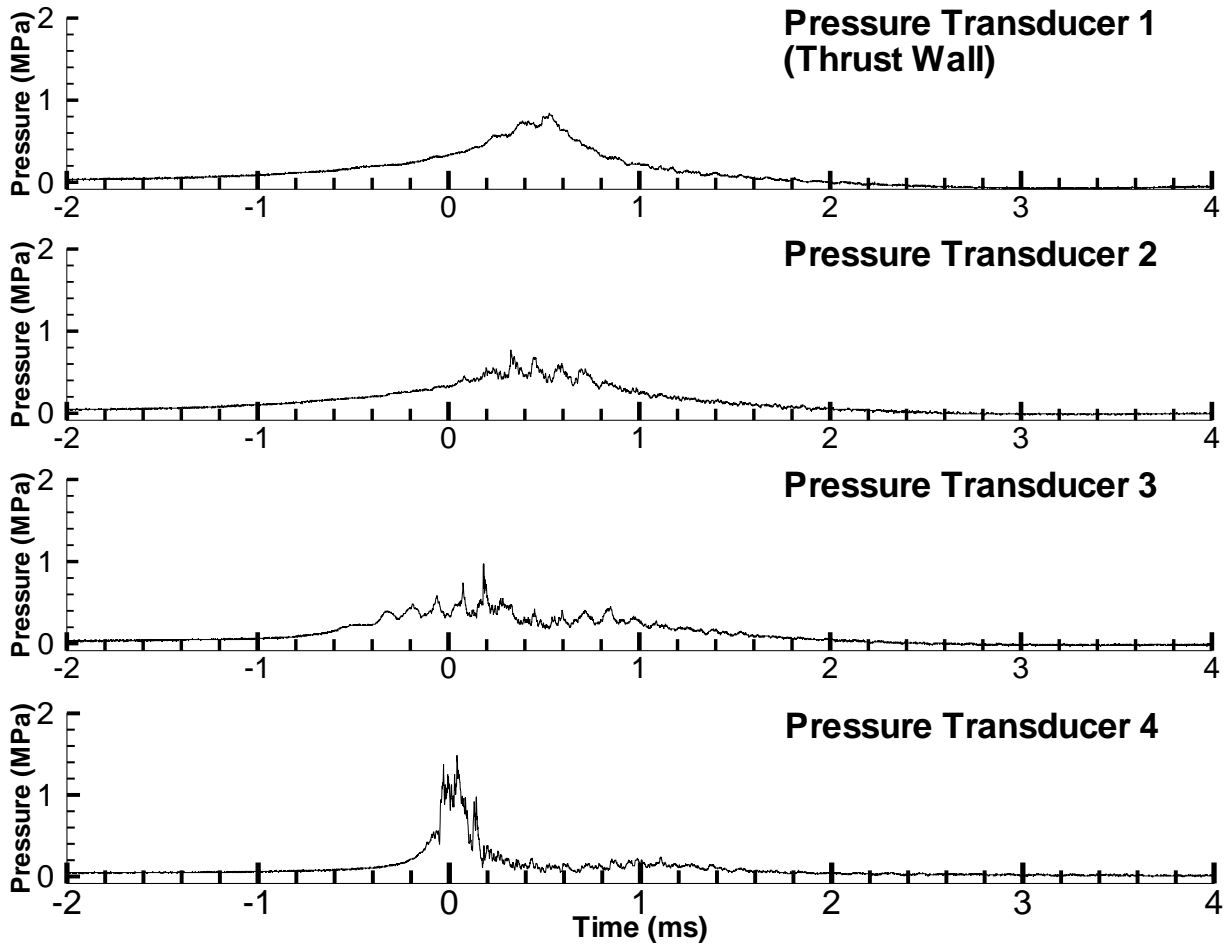


Figure 9: Cooper et al.



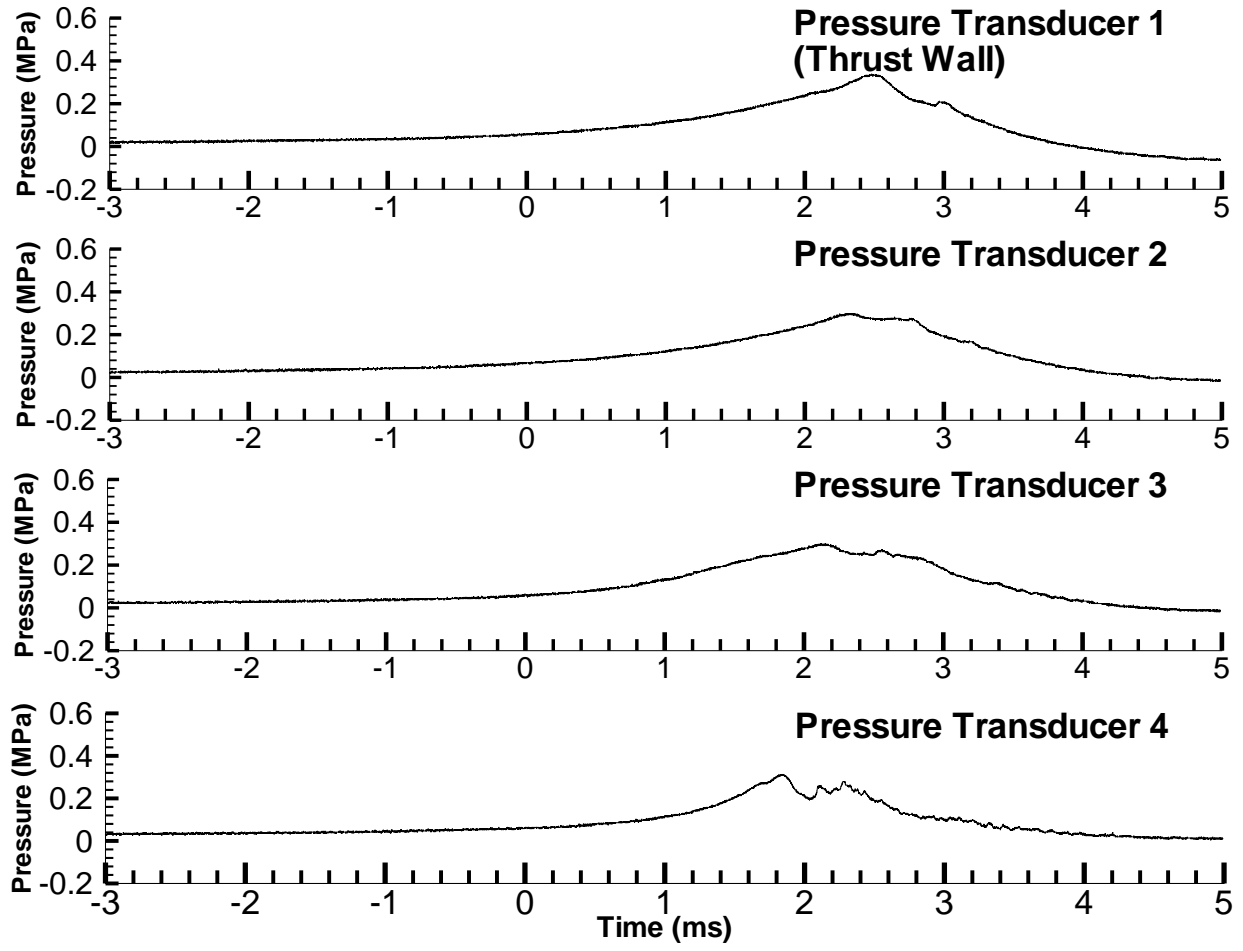


Figure 10: Cooper et al.

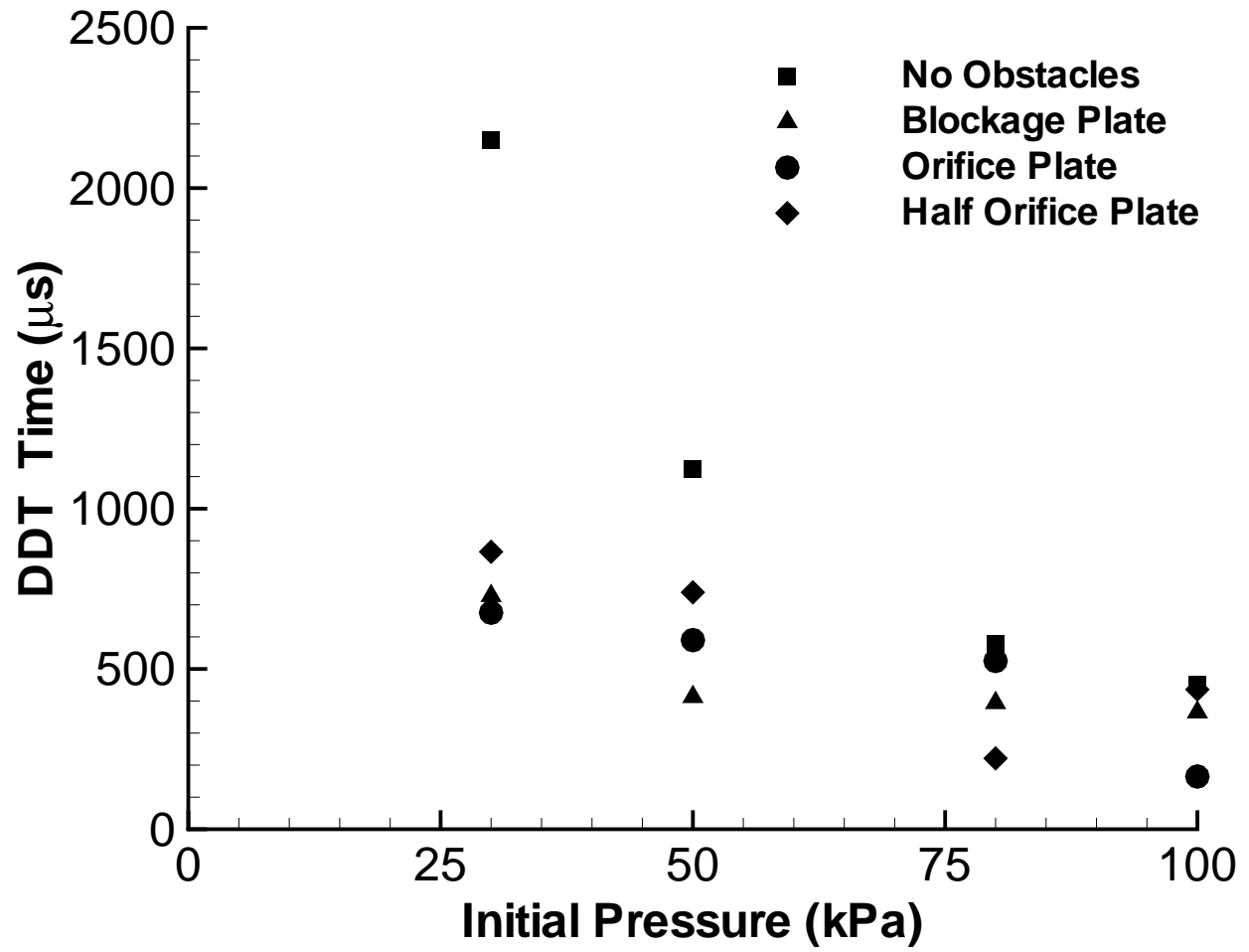


Figure 11: Cooper et al.

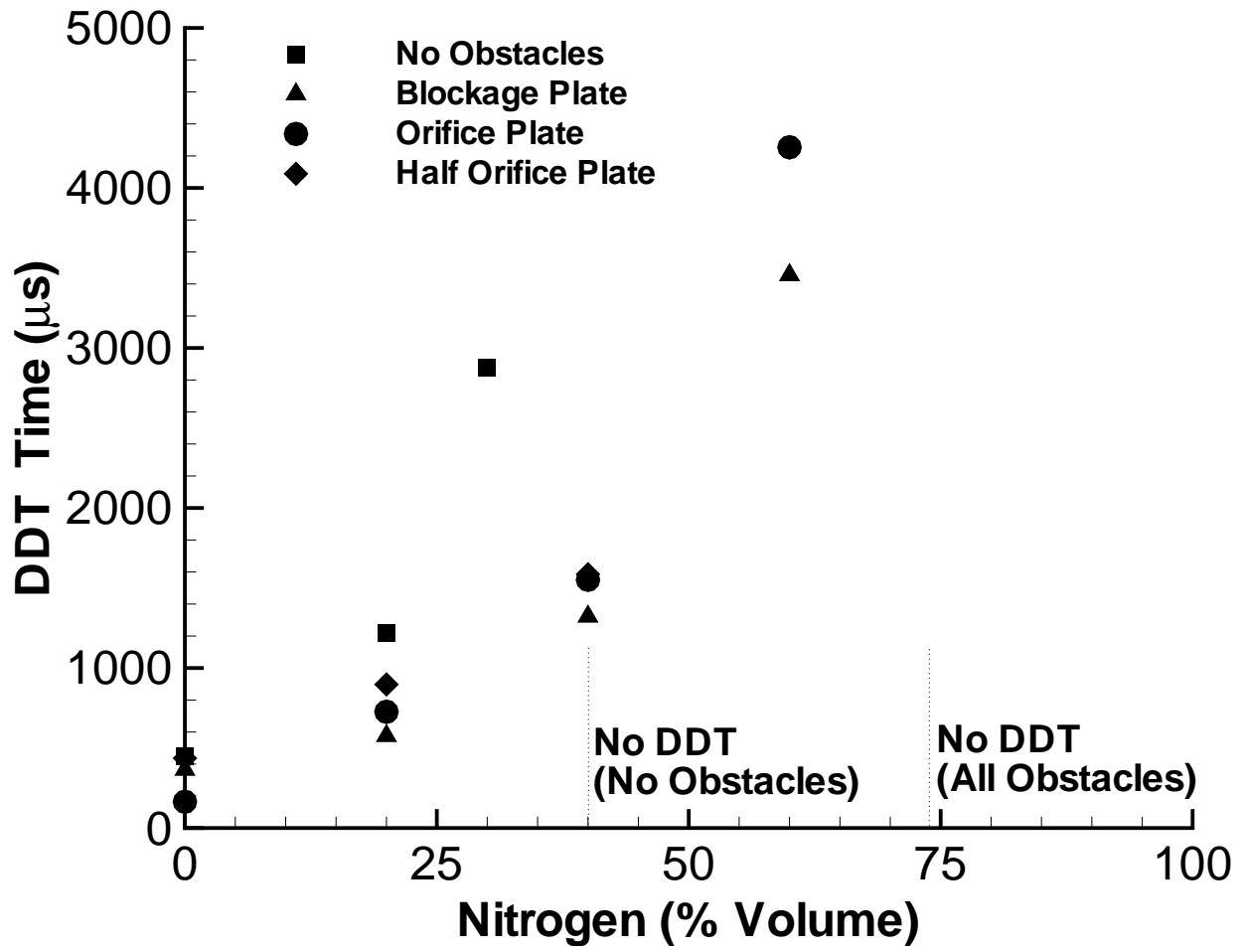


Figure 12: Cooper et al.

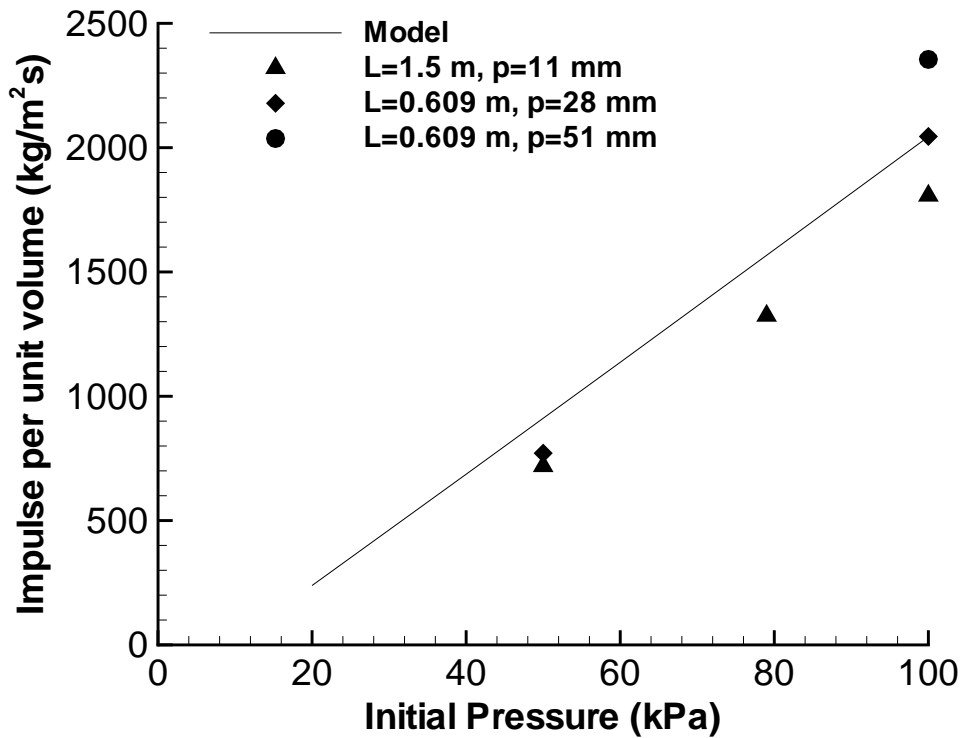
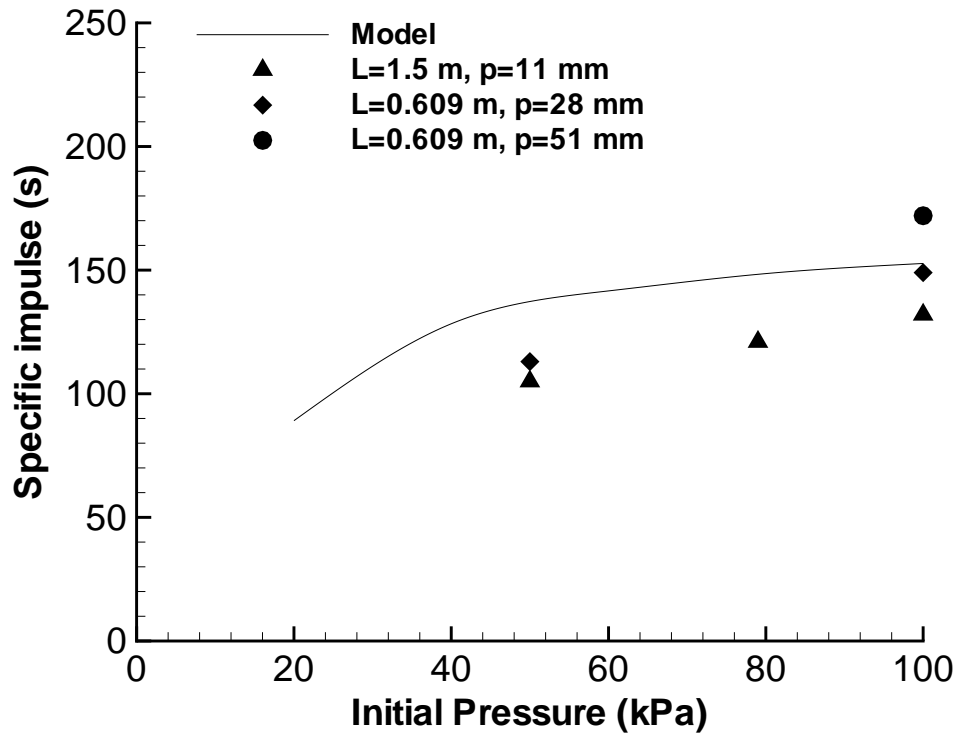


Figure 13: Cooper et al.

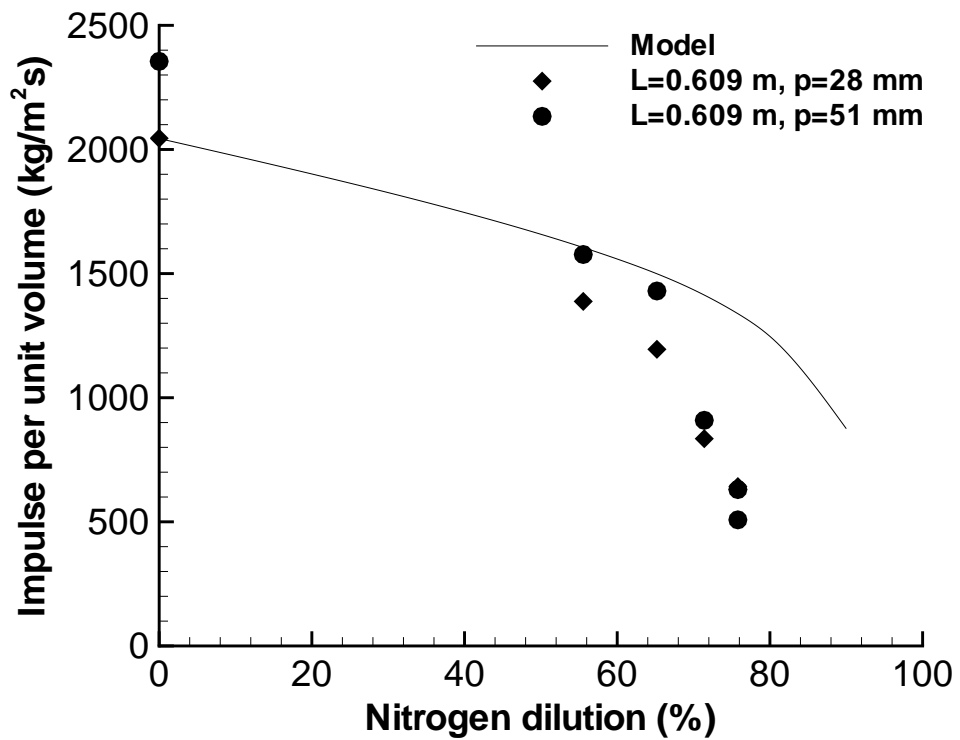
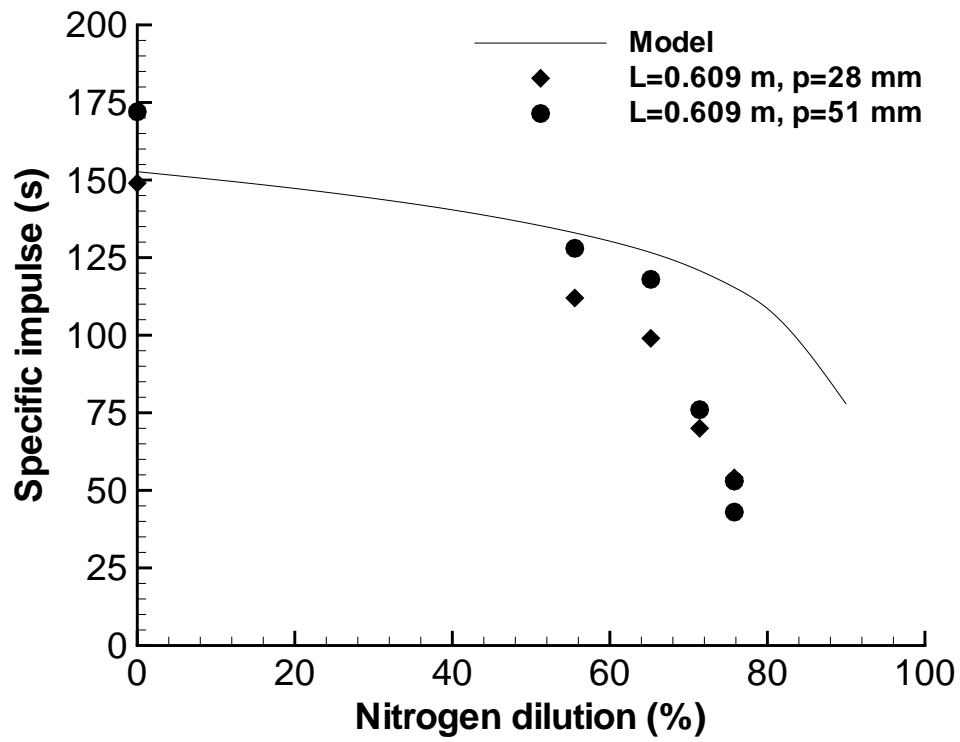


Figure 14: Cooper et al.

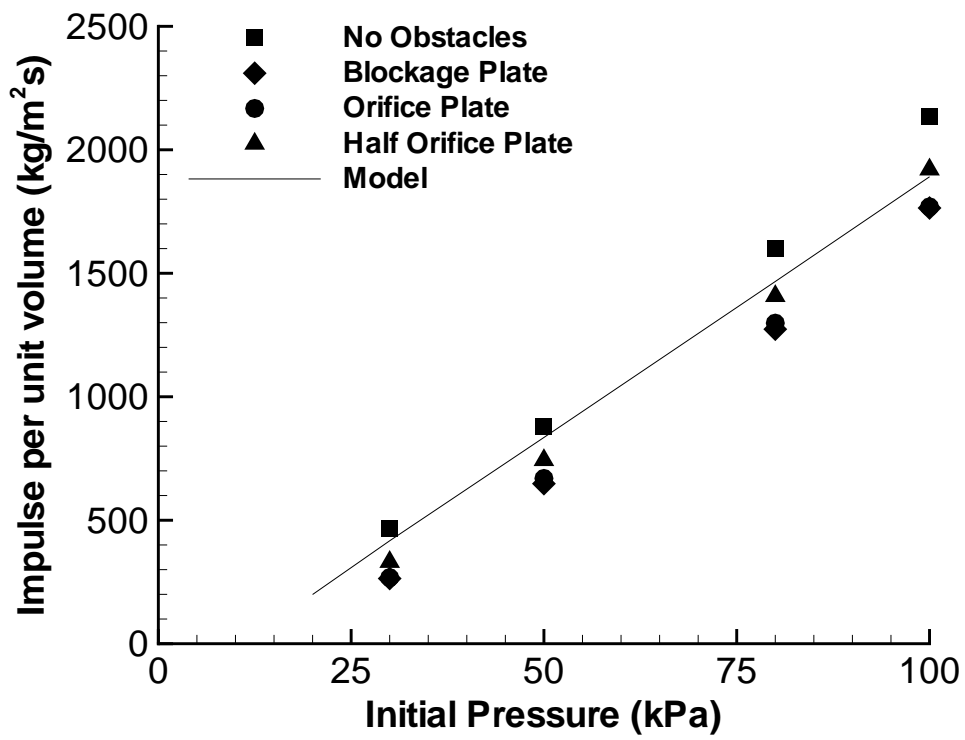
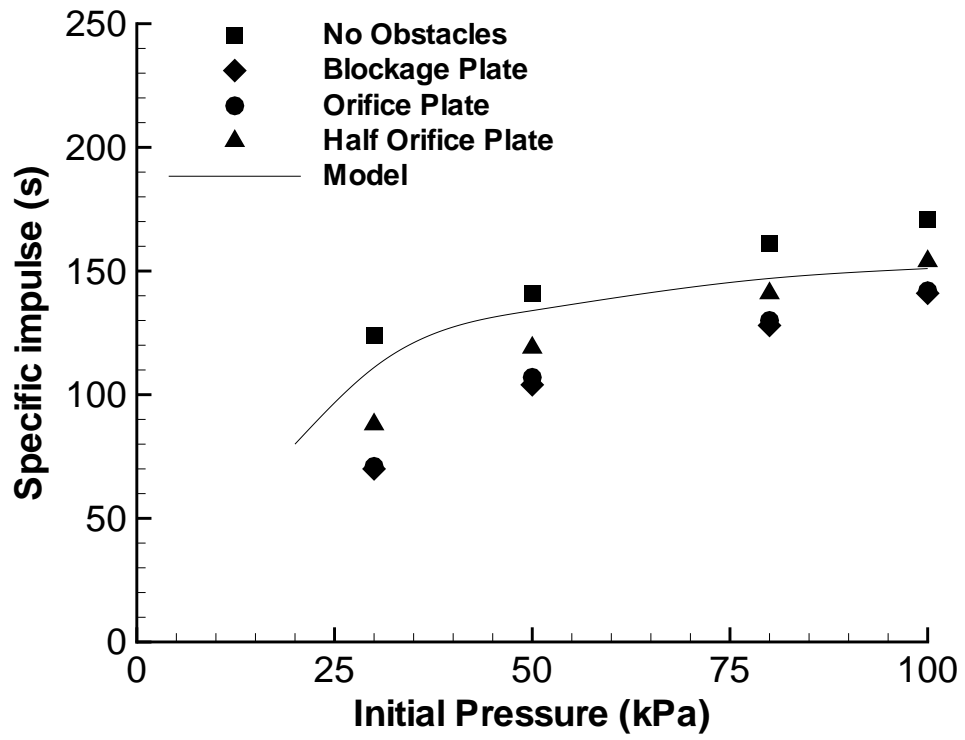


Figure 15: Cooper et al.

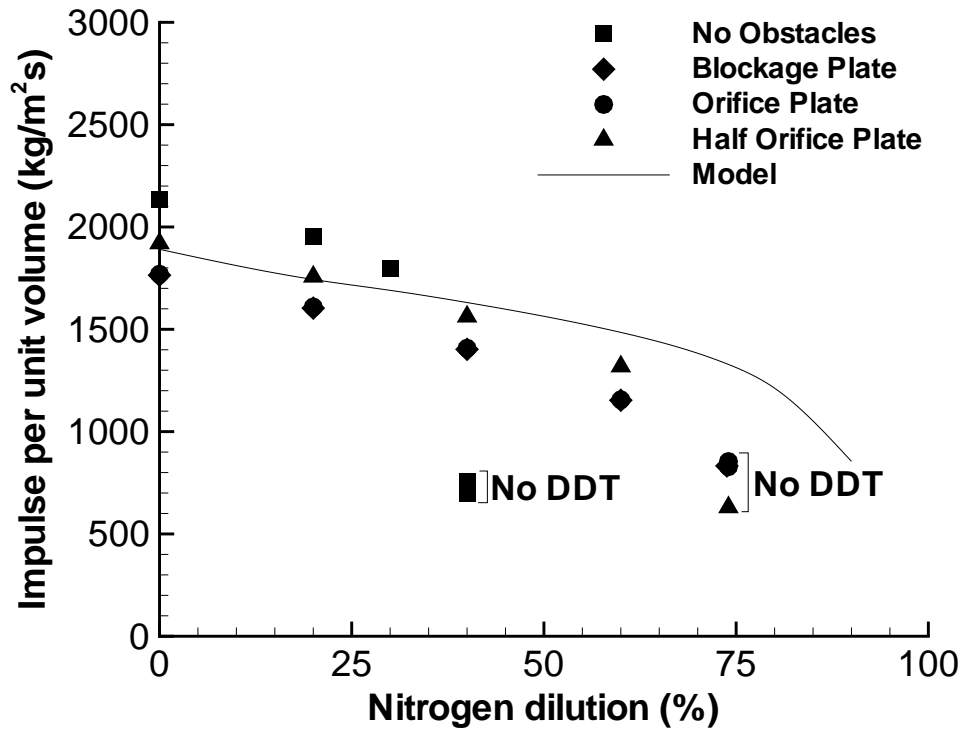
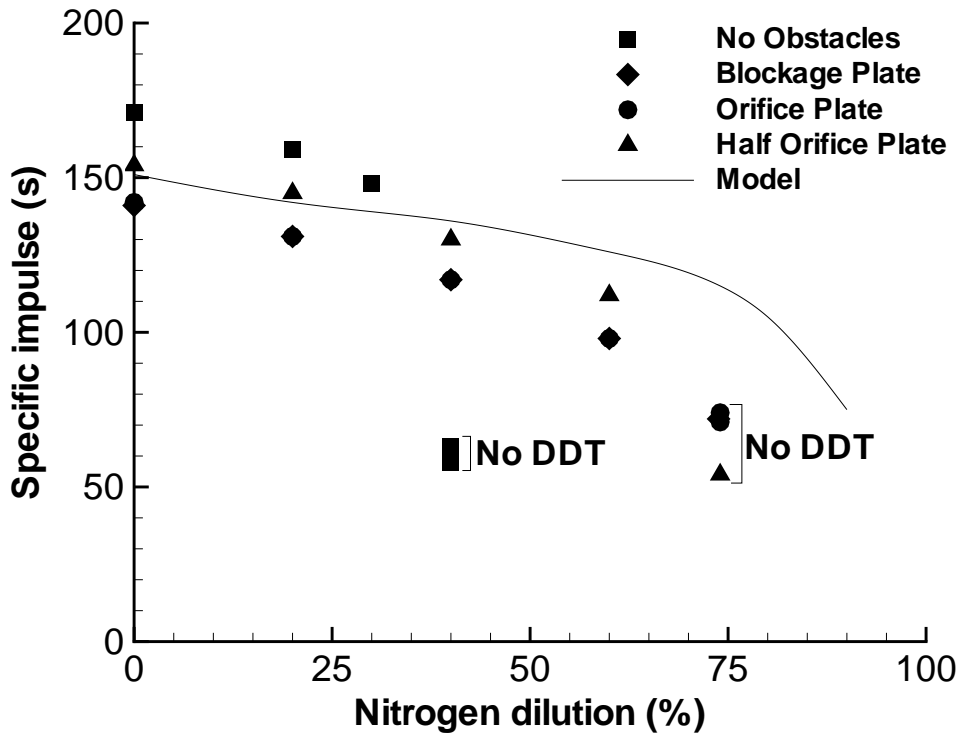


Figure 16: Cooper et al.

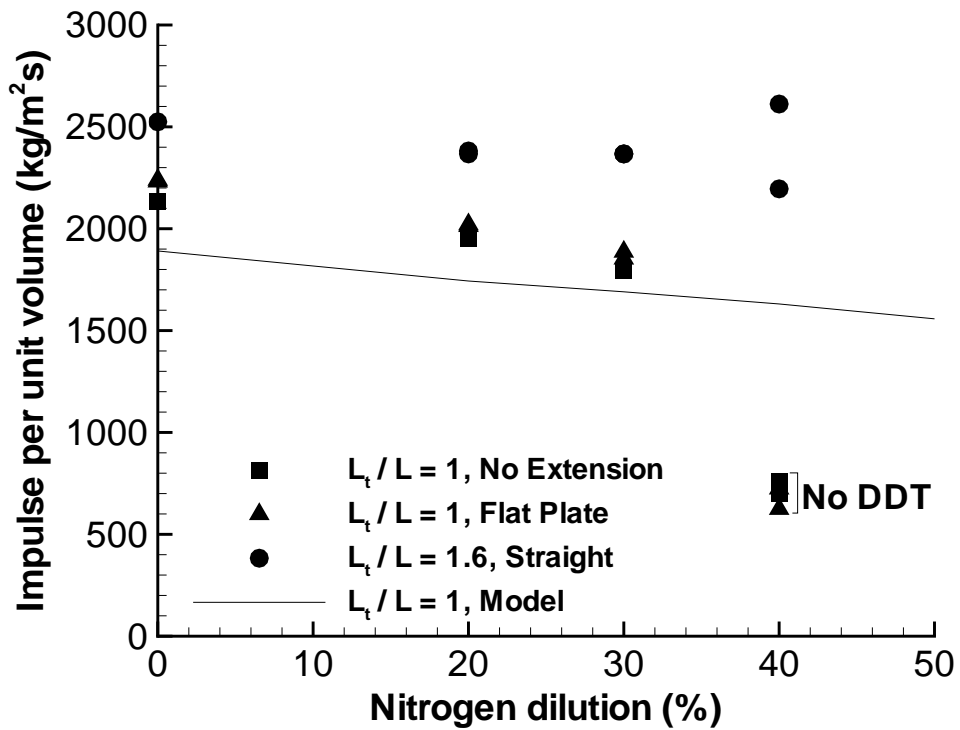
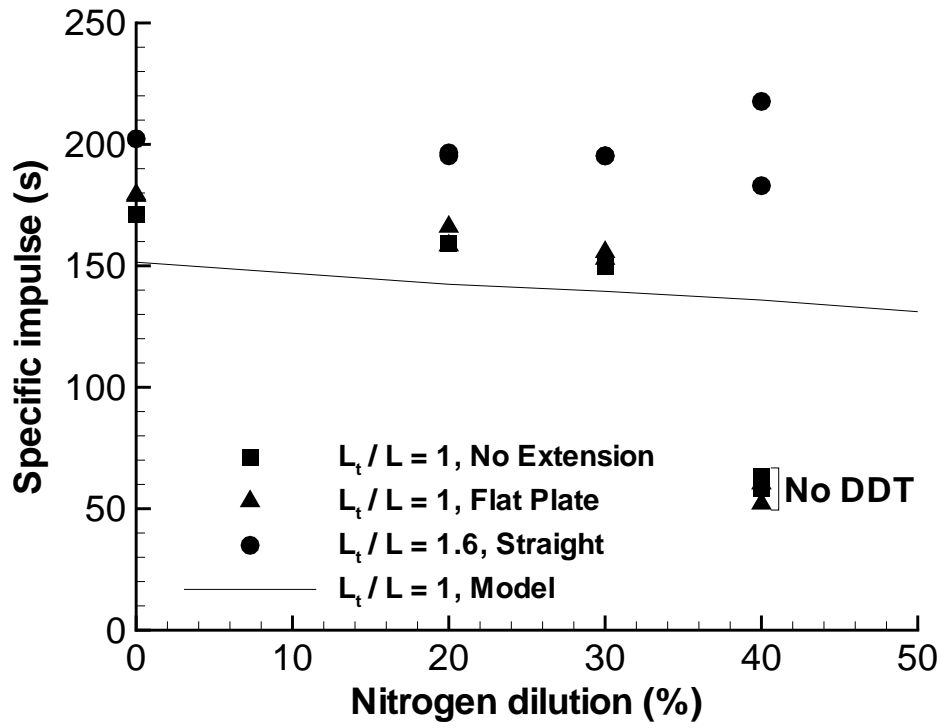


Figure 17: Cooper et al.



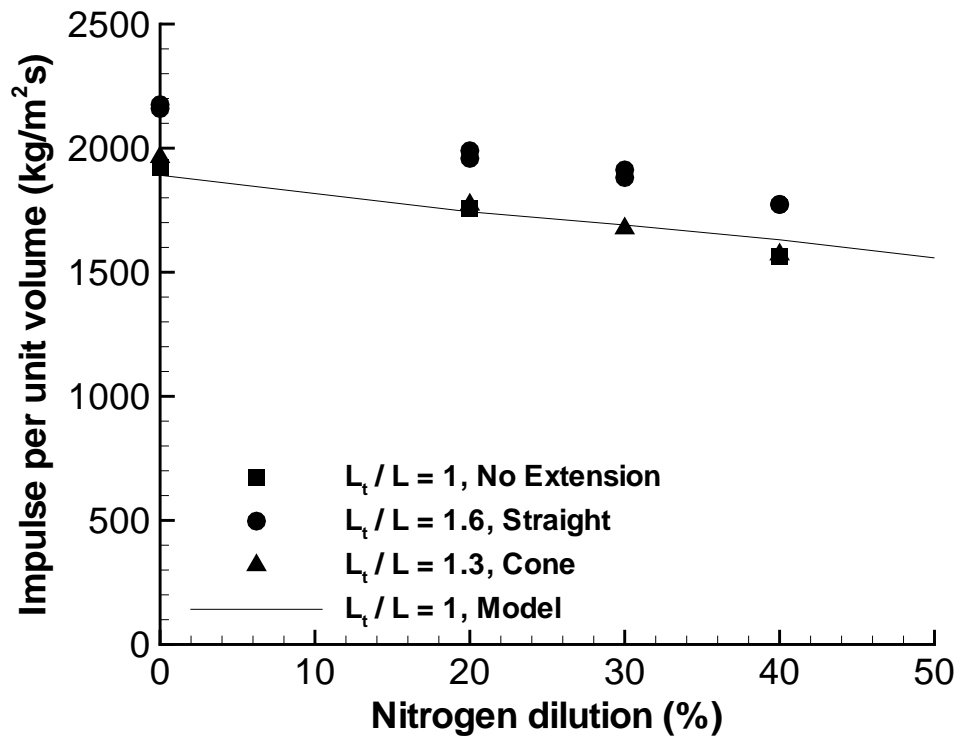
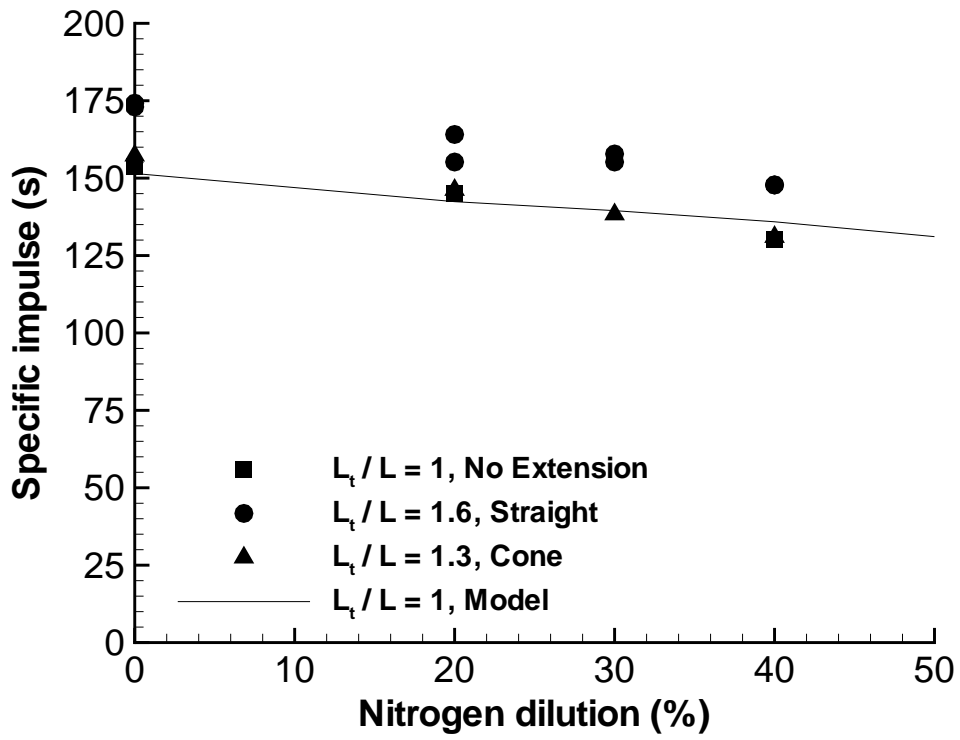


Figure 18: Cooper et al.